JOURNAL OF Applied Polymer SCIENCE

Preparation and Use of Magnetic Poly(glycidyl methacrylate) Resin in Drinking Water Treatment

Wei Chen, Yu Liu, Cheng Liu
Environment College, Hohai University, No.1 Xikang Road, 210098, Nanjing, China
Correspondence to: C. Liu (E-mail: liucheng8791@hhu.edu.cn)

ABSTRACT: Magnetic poly(glycidyl methacrylate) (m-PGMA) was synthesized and characterized, and its efficiency in removing natural organic matter (NOM) and carbamazepine (CBZ) from synthetic water was studied. The effects of factors such as time and m-PGMA dosage on NOM removal were investigated. Furthermore, magnetic ion exchange resin (MIEX®) was used for comparison with m-PGMA in CBZ removal. m-PGMA was found to have a strong magnetic character whose specific saturation magnetization and mass fraction of magnetite were 10.79 emu g^{-1} and 6.166 wt %, respectively, thus providing additional utility for m-PGMA in slurry form in completely mixed continuous-flow reactors. Lab-scale studies showed that the removal rate rose rapidly with time and reached a pseudo-equilibrium after 30 min. In addition, the highest doses of m-PGMA achieved the highest removal efficiency. After 30 min of contact with 5, 10, and 15 mL L^{-1} of m-PGMA, the removal rates, based on UV absorbance measurements at 254 nm (UV_{254}), were 56%, 67%, and 79%, respectively, whereas the removal rates of dissolved organic carbon (DOC) were 53%, 60%, and 72%, respectively. Additionally, the scale ultraviolet absorbance values (SUVA) decreased during a 30 min contact time, thereby suggesting that the NOM removed by m-PGMA had greater aromatic character. In multiple-loading tests, UV_{254} removal gradually decreased and achieved 18.39% at 1600 bed volume; it was kept constant at this level. Compared to MIEX®, m-PGMA had a higher CBZ removal rate (27.8% and 34.7% for 20 mL L^{-1} and 25 mL L^{-1} of m-PGMA, corresponding to the removal of 200 μg L^{-1} CBZ). The resulting higher removal rate of CBZ contributed to stronger adsorption, a higher specific surface area, and larger pore volume.

KEYWORDS: magnetism and magnetic properties; resins; applications

Received 22 October 2012; accepted 3 February 2013; published online 8 March 2013
DOI: 10.1002/app.39117

INTRODUCTION

Natural organic matter (NOM) is ubiquitously present in drinking water sources and plays an important role in drinking water treatment processes.[1–3] NOM is known to increase the demand for disinfectants and coagulants,[4] to generate potentially harmful disinfection byproducts[5] and foul membranes,[6] and to facilitate bacterial reproduction during drinking water distribution.[7] Therefore, different methods have been employed to remove NOM from source water, such as enhanced coagulation,[8] membrane separation,[9] and chemical oxidation. Unfortunately, these methods pose different challenges. For example, coagulation removed 60% of the dissolved organic carbon (DOC) associated with the 1–10,000 fraction but had little impact on the DOC concentration of the <1000 fraction.[10] NOM removal rates by ultrafiltration (UF) membranes typically only range from 10% to 50%.[11,12] Chemical oxidation for the complete mineralization of NOM is usually expensive. Moreover, all of these methods consume energy (radiation, ozone, etc.) and chemical reagents (e.g., catalysts and oxidizers), the amounts of which increase with treatment time.[13]

In recent years, an anion exchange resin (AER) has been evaluated for its efficiency at removing NOM.[7,14,15] Magnetic ion exchange resin (MIEX®), which was developed as a new version of AER, has three main characteristics. First, the magnetic component added to MIEX® can achieve effective solid–liquid separation.[10] Thus, MIEX® was designed for use in slurry form in completely mixed continuous-flow reactors.[15] Second, MIEX® has rapid exchange kinetics, because it is two to five times smaller than conventional AER, thus providing a greater external surface area (SA).[6] Finally, MIEX® is an alternative pretreatment method for coagulation, membrane separation, and active carbon adsorption due to its high and rapid removal rate of NOM. For instance, MIEX® removed approximately 80% of the DOC associated with the 1–10,000 ultrafiltration fraction and almost 60% of the DOC associated with the <1000 ultrafiltration fraction, of which hardly any was removed by coagulation.[10,16] When used as a pretreatment process for microfiltration, MIEX® removed a significant amount of organic matter in raw water, thus reducing

Additional Supporting Information may be found in the online version of this article.

membrane fouling.[17] Moreover, a combination of MIEX® and powered activated carbon lowered the competitive adsorption between NOM and trace organic compounds.[7,18]

Pharmaceutical residues have been reported to be present in wastewater treatment plants, ground water, rivers, and reservoirs at concentrations up to the $\mu g\ L^{-1}$ level.[19,20] Likewise, both pharmaceutical residues and personal care products (PPCPs) have been detected in the Yellow River and in the Pearl River basin, with concentrations ranging from ng L^{-1} to $\mu g\ L^{-1}$.[21] However, MIEX® exhibited a poor removal rate for electrically neutral trace organic matter such as atrazine, which is representative of PPCPs,[22] because ion exchange is ineffective at removing neutral trace organic matter. Adsorption was shown to be a preferable method for removing pharmaceutical residues, because it does not produce undesirable byproducts and is easy to run.[23] Consequently, the development of a magnetic, strong AER with a well-developed pore structure and a high specific SA, which would not only remove NOM but also remove electrically neutral PPCPs, has research significance.

In this article, we focused on preparing and characterizing a magnetic poly(glycidyl methacrylate) (m-PGMA) bead that can be used in slurry form due to its magnetic core. The diameter of the m-PGMA beads was approximately 100–200 μm, thus providing a greater external SA. Moreover, a mixed porogen was added during synthesis of m-PGMA to obtain a well-developed pore structure and a high specific SA. The ability of m-PGMA to remove NOM and carbamazepine (CBZ), one of the most frequently detected pharmaceutical residues in aquatic environments, was evaluated by conducting lab-scale experiments.[24,25]

EXPERIMENTAL

Materials

Magnetite (Fe_3O_4) particles were submicron-sized. Oleic acid (CANSPEC, Shanghai, China) was used to modify the surface of the as-received magnetite. Glycidyl methacrylate (GMA; CANSPEC, Shanghai, China) was used as a basic monomer after filtration using an inhibitor remover. Divinylbenzene (DVB; CANSPEC, Shanghai, China) was used after the removal of inhibitors. Azobisisobutyronitrile (AIBN; CANSPEC, Shanghai, China) was used as a radical initiator for the reaction. Polyethylene Glycol 6000 (PEG; CANSPEC, Shanghai, China) was used as a dispersing agent. Methylbenzene (CANSPEC, Shanghai, China), cyclohexanone (CANSPEC, Shanghai, China), and atoleine (CANSPEC, Shanghai, China) were used as porogens. Trimethylammonium chloride (CANSPEC, Shanghai, China) was used in a quaternization reaction. Absolute ethyl alcohol, methylcellulose solution with a mass concentration of 0.1%, and NaCl solution with a mass concentration of 5% were used. Two synthetic water samples, (a) and (b), were prepared: (a) with NOM (CANSPEC, Shanghai, China) for which the UV_{254} and DOC were approximately 0.378 abs and 3 mg L^{-1}, respectively, and (b) with CBZ (CANSPEC, Shanghai, China) at a concentration close to 200 $\mu g\ L^{-1}$.

Preparation of m-PGMA

Grafting of Oleic Acid onto the Surface of Magnetite. Magnetite (32.22 g) was soaked with oleic acid (3 g) in absolute ethyl alcohol (100 mL), and the solution was rapidly stirred at 50°C for 5 h. Precipitated magnetite was immobilized with a permanent magnet, and the aqueous supernatant was decanted and discarded. The oleic-acid-grafted magnetite was then dried at 40°C. The dried oleic-acid-grafted magnetite was mixed with Polyethylene Glycol 6000 (50 g) in distillate water (100 mL), and the solution was ultrasonically processed for 1 h. The final product was a suspension of oleic-acid-grafted magnetite–Polyethylene Glycol.

Suspension Polymerization. The oleic-acid-grafted magnetite–Polyethylene Glycol suspension, distillate water (60 mL), and absolute ethyl alcohol (40 mL) were mixed and decanted into a three-necked flask that was equipped with a stirrer and a Graham condenser. The mixture was rapidly stirred at 65°C for 10 min. Then, GMA (50 mL), DVB (25.35 g), AIBN (6 g), 5% NaCl solution (25 mL), 0.01% methylcellulose (MC) solution (25 mL), methylbenzene (27.4 g), cyclohexanone (4.8 g), and atoleine (8.1 g) were mixed and carefully added to the three-necked flask with continuous stirring. To obtain magnetic polymer microspheres, suspension polymerization was performed at 75°C for 1.5 h and then at 80°C for 0.5 h. After the suspension polymerization was complete, the product was washed with excess tepid distillate water and extracted with a Soxhlet extractor with methyl alcohol for 12 h to remove remaining porogens and the nonencapsulated magnetite. The product was dried at 40°C, and the final product was sieved consecutively through 200-μm and 100-μm strainers.

Quaternization with Trimethylammonium Chloride for m-PGMA. Dried magnetic polymer microspheres mixed with 50% trimethylammonium chloride solution ($m_{\text{magnetic polymer microspheres}} : m_{\text{trimethylammonium chloride}} = 1 : 2.5$) were decanted into a three-necked flask. The solution was stirred at 80°C for 10 h. The final product was first washed with excess 1 M HCl solution and then washed with excess distillate water until the supernatant was pH 7. The chemical equations for synthesizing m-PGMA and the segment unit model of m-PGMA are provided in Figure 1.

Evaluating Removal Rate to NOM and CBZ of m-PGMA

Kinetic Tests. In the kinetic tests, glass beakers were filled with 1 L of unfiltered synthetic water (a), placed on the jar tester, dosed with m-PGMA, and mixed at 200 rpm for 120 min at a solution temperature of 20 ± 2°C. Samples were withdrawn from the beakers at predetermined time intervals (10, 20, 30, 40, 50, 60, 80, 100, and 120 min) and filtered through polyether sulfone filter papers (0.45 μm) for further DOC and UV_{254} absorbance measurements. All measurements were conducted either in duplicate or in triplicate, and the jar tests were conducted in parallel. The tested doses of m-PGMA in separate beakers were 5, 10, and 15 mL of settled resin for synthetic water (a).

Multiple-Loading Jar Tests. In the multiple-loading jar tests, the beaker was initially filled with 1 L of unfiltered synthetic water (a) dosed with 10 mL L^{-1} of m-PGMA and then mixed at 200 rpm at 20 ± 2°C for 30 min. This first step represented a loading of 100 bed volume (BV), comparable to a treated water volume 100 times that of the m-PGMA dosed water. After 30 min of mixing and 3 min of settling, samples were taken

Applied Polymer SCIENCE

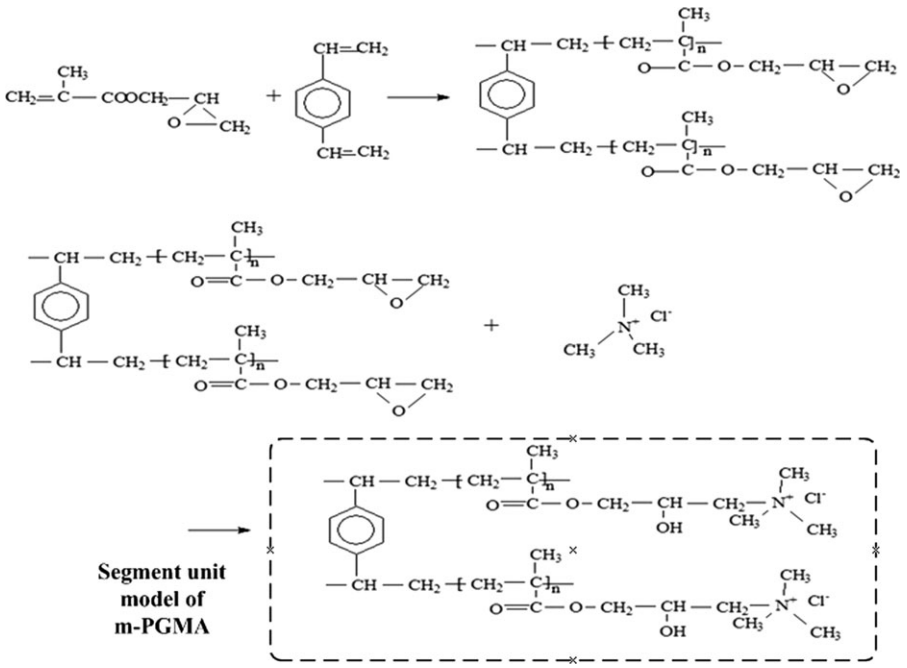

Figure 1. The chemical equations for synthesizing m-PGMA and the segment unit model of m-PGMA.

from the supernatant and filtered prior to the DOC and UV_{254} absorbance measurements. The remaining unfiltered supernatant was carefully decanted, leaving a settled m-PGMA volume of approximately 10 mL in the beaker. For the second and all subsequent loading steps, the beaker containing settled m-PGMA was again filled with 1 L of synthetic water (a) and stirred for 30 min at 200 rpm. The same scheme was employed until a loading of 2700 BV was achieved. The series was performed in one step without interruptions. Samples were withdrawn from the beakers and filtered with polyether sulfone filter papers (0.45 μm) prior to further UV_{254} absorbance measurements.[26]

Comparing Removal Rate to CBZ of m-PGMA and MIEX®

The glass beakers were filled with 1 L of unfiltered synthetic water (b) and placed on the jar tester. m-PGMA and MIEX® were added at concentrations of 20 mL L^{-1} and 25 mL L^{-1}, respectively, and then mixed at 200 rpm for 30 min and allowed to settle for 3 min at a solution temperature of 20 ± 2°C. Samples were taken from the supernatant and filtered prior to CBZ residue analysis.

Characterization

The surface functional groups of oleic-acid-grafted magnetite and m-PGMA were confirmed through diffuse-reflectance Fourier Transform infrared spectroscopy (FTIR) (IRAffinity-1). The powder samples were ground with KBr and compressed into a pellet whose spectra were recorded. The size distributions of oleic-acid-ungrafted and oleic-acid-grafted magnetite were determined by a nanometer laser particle size analyzer (Zetasizer Nano S90). The magnetite was dispersed in absolute ethyl alcohol and measured in a quartz cuvette. The magnetic substance content of m-PGMA was measured by thermogravimetric analysis (TGA; Netzsch TG). The sample was centrifuged to remove surface water, and then the sample was heated from room temperature to 600°C at a rate of 5°C min^{-1}. Meanwhile, weight loss as a function of increasing temperature was recorded to construct a thermogravimetric curve. The magnetic properties of m-PGMA were determined with a vibrating sample magnetometer (Lakeshore 7300) for the powders at room temperature. Nitrogen adsorption analysis was carried out using a Belsorp-mini apparatus at −196°C. Samples were degassed overnight at 200°C under nitrogen flow prior to the measurements. The specific SA was calculated using the Brunauer–Emmett–Teller (BET) method, with a P/P_0 range between 0.0 and 0.5. The pore volume (PV) was calculated from the adsorption isotherm at a relative pressure of 0.99, and the average pore diameter (APD) was determined from either the adsorption branch or the desorption branch of the isotherm hysteresis using the Barrett–Joyner–Halenda method. The base anion exchange capacity of m-PGMA was measured using the method recommended by the Orica® Company.

The UV_{254} absorbance (in triplicate) of the water samples was measured by a UV–visible spectrophotometer (UV-1601, Shimadzu). DOC analysis was performed with a total organic carbon (TOC) analyzer (TOC-5000A, Shimadzu) using a high temperature combustion method. The minimum detection limit of the DOC analyzer was 0.1 mg L^{-1}. The CBZ content was determined by high-performance liquid chromatography (SHIMADZU LC-20AT).

RESULTS AND DISCUSSION

Characterization of m-PGMA

FTIR Spectra of the Magnetite and m-PGMA. A comparison of the FTIR spectra of pure magnetite (a), oleic-acid-coated magnetite (b), and m-PGMA (c) is shown in Figure 2. In Figure 2(a), the characteristic absorption bands of the Fe–O bond

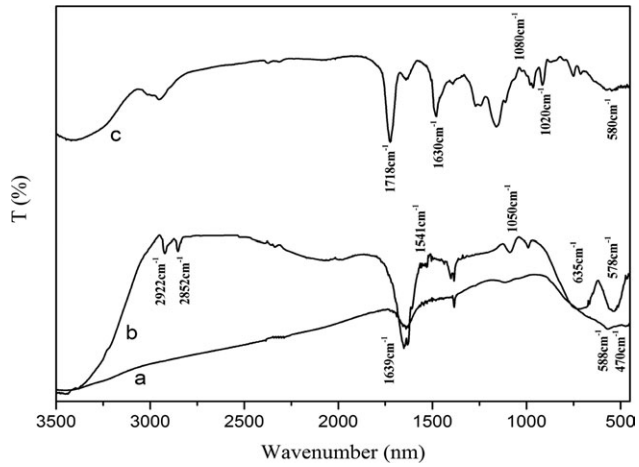

Figure 2. FTIR spectra of (a) pure magnetite, (b) magnetite coated with oleic acid (OA), and (c) m-PGMA.

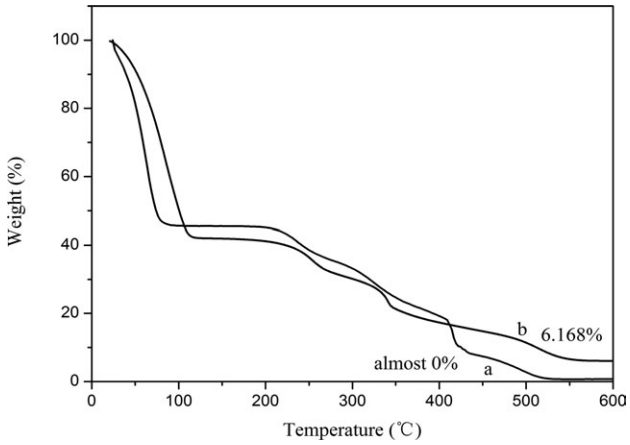

Figure 3. The weight loss as function of temperature for (a) PGMA and (b) m-PGMA.

appear at approximately 635 cm^{-1} and 578 cm^{-1}, because the size of the magnetite particles decreased to nanoparticles.[27,28] The sizes of the oleic-acid-ungrafted and oleic-acid-grafted magnetite are presented in Figure S1 (Supporting Information). In curve (b), two sharp bands at 2922 cm^{-1} and 2855 cm^{-1} are attributed to the stretching of asymmetric and symmetric CH_2 moieties, respectively. Moreover, two new bands appear at 1541 cm^{-1} and 1639 cm^{-1} that are characteristic of the asymmetric ν_{as}(COO–) and the symmetric ν_s(COO–) stretching.[29] A strong absorption at 1050 cm^{-1} resulted from C–O single bond stretching.[27] The existence of a carboxyl peak indicated that oleic acid was indeed adsorbed to the magnetite. In curve (b), the characteristic absorption peak of a benzene ring was found at 1630 cm^{-1}, thus confirming that DVB was involved in the reaction. The ester carbonyl was identified with a strong stretching band at 1718 cm^{-1}, whereas the –OH of water adsorbed to m-PGMA resulted in a broad stretching band near 3500–3300 cm^{-1}. Furthermore, medium stretching bands at 1020 cm^{-1} and 1080 cm^{-1} were attributed to quaternary ammonium moieties in m-PGMA.[30] The existence of quaternary ammonium groups demonstrated that m-PGMA is a type of AER.

TGA of m-PGMA. The amount of containment for magnetite in the m-PGMA was evaluated by TGA. m-PGMA completely decomposed above 600°C but left a residual mass of approximately 6.168 wt %, which was equal to the mass of the magnetic part [Figure 3(b)]. However, as shown in Figure 3(a), PGMA without magnetite was completely decomposed at 600°C and left almost 0 wt % residual mass. All of the monomer and active groups disintegrated completely at 600°C except for the magnetic part, because ferroferric oxide is more likely to oxidize (thus forming iron sesquioxide) than to disintegrate.

Magnetization of m-PGMA. Figure S2 shows that the specific saturation magnetization of m-PGMA was approximately 10.79 emu g^{-1} at room temperature, whereas the coercivity and remanence of m-PGMA were negligible. Moreover, m-PGMA is highly sensitive to an external magnetic field and can easily be magnetized and demagnetized.

Specific SA and Pore Structure Characteristic of m-PGMA and MIEX®. Table I, Figure S3, and Figure S4 display the pore size distribution, pore structure characteristics, and specific SA of both m-PGMA and MIEX®. As seen in Table I, the specific SA, total PV, and APD of m-PGMA are 40.026 m^2 g^{-1}, 0.1852 cm^3 g^{-1}, and 18.509 nm, whereas the values for MIEX® are 4.341 m^2 g^{-1}, 0.018408 cm^3 g^{-1}, and 16.962 nm, respectively. As shown in Figures S2 and S3, the pore size distribution of m-PGMA is narrow and centered around 10 nm, whereas MIEX® has a wider pore size distribution. The higher specific SA of m-PGMA occurred due to the addition of a mixed porogen consisting of a good solvent and a poor solvent. A cross-linked copolymer was dissolved and inflated in the good solvent (methylbenzene), whereas atoleine and cyclohexane, used as poor solvents, were insoluble in the interior of the resin, thus producing phase separation followed by the creation of pores from subsequent fluid flow.

From the above characterization of m-PGMA, we can draw several conclusions as follows. First, chloride ions in the segment unit model of m-PGMA can exchange with negatively charged NOM. Moreover, the TGA results and the specific saturation magnetization of m-PGMA show that m-PGMA can be magnetically separated in water. Finally, m-PGMA, which is similar to MIEX®, is a small bead measuring approximately 100–200 μm in diameter. Therefore, m-PGMA can be used in slurry form in completely mixed continuous-flow reactors. Moreover, m-PGMA has a rapid solid–liquid separation rate, and following reaction, m-PGMA can rapidly isolate itself from water to regenerate.

Table I. Pore Construction Characteristic and Specific SA of m-PGMA and MIEX®

	$a_{s,BET}$ (m^2 g^{-1})	Total PV (P/P_0 = 0.990; cm^3 g^{-1})	APD (nm)
m-PGMA	40.026	0.1852	18.509
MIEX®	4.341	0.018408	16.962

Applied Polymer SCIENCE

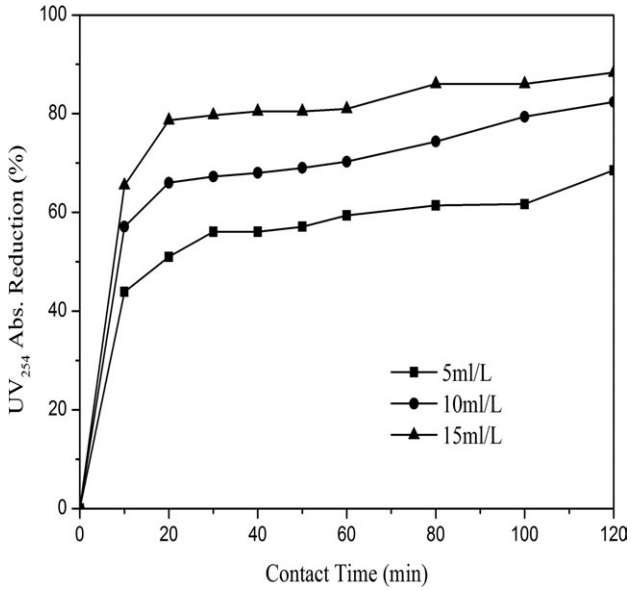

Figure 4. The impacts of m-PGMA dose and contact time on UV_{254} absorbance reduction in kinetic tests of synthetic water (a).

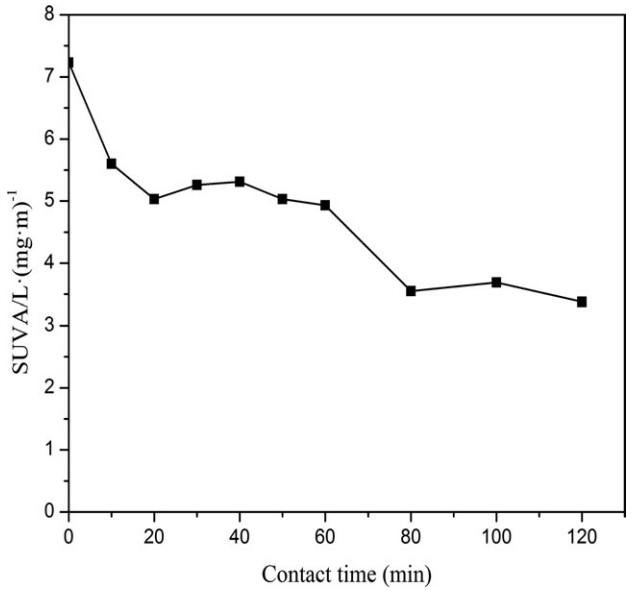

Figure 6. Residual SUVA of synthetic water (a) treated by m-PGMA (resin dose: 15 mL L^{-1}).

Removal Rate of NOM and Trace Organic Matter by m-PGMA

Removal Rate of NOM by m-PGMA. *Kinetic tests.* The kinetics of DOC and UV_{254} removal treated with different resin doses of m-PGMA for synthetic water (a) are plotted in Figures 4 and 5. The results indicated that the majority of removal for both the UV_{254} and DOC methods occurred in the first 20–30 min of mixing, and they reached a maximum (pseudo-equilibrium) after 30 min of contact time. Additional results indicated that higher m-PGMA doses generally resulted in greater UV_{254} and DOC removal after 120 min of contact time. Consequently, the UV_{254} absorbance reduction increased to 56%, 67%, and 79% for 5, 10, and 15 mL of settled resin L^{-1}, respectively, and the DOC reduction increased to 53%, 60%, and 72% for 5, 10, and 15 mL of settled resin L^{-1}, respectively. We believe that dissolved organic matter (DOM) that is part of NOM is rich in carboxylic acid functional groups, which gives DOM a net negative charge over the pH range of natural water and allows DOM to take part in anion exchange reactions.[31,32] Moreover, similar to MIEX®, m-PGMA is composed of small beads and can be used in suspension in a completely mixed flow reactor. The increased SA of m-PGMA causes turbulence around the resin and decreases resistance to liquid-phase mass transfer.[6,14] Therefore, m-PGMA has a faster removal rate for NOM compared with traditional ion exchange resins.

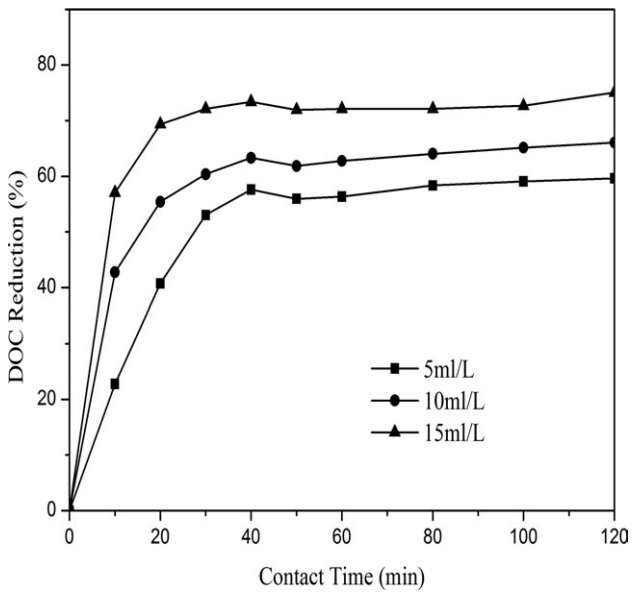

Figure 5. The impacts of m-PGMA dose and contact time on DOC reduction in kinetic tests of synthetic water (a).

The scale ultraviolet absorbance (SUVA) for synthetic water (a) prepared in lab, as a function of contact time with m-PGMA (15 mL L^{-1}), is shown in Figure 6. SUVA is the ratio of UV_{254} to DOC multiplied by 100, and it tends to be strongly correlated with the aromatic carbon content of NOM in water.[17] In summary, water with high SUVA is characterized by hydrophobic NOM and low ionic strength, whereas water with low SUVA has hydrophilic NOM.[15] As shown in Figure 6, SUVA values were reduced by more than 50% with m-PGMA after a pseudo-equilibrium resulted in the preferential removal of NOM with a higher aromatic character. In accordance with previous work, aromatic moieties were found to be preferentially removed by AERs.[7,22] m-PGMA is a type of AER. In addition, we tentatively hypothesize that m-PGMA and MIEX® possess similar polyacrylic backbones that have affinity for aromatic fractions.

Multiple-loading tests. The aim of the multiple-loading tests was to estimate the performance of a continuously operated m-PGMA process using the same resin multiple times without regeneration. UV_{254} absorbance removals in multiple-loading jar tests for synthetic water (a) are illustrated in Figure 7. At 100 BV loading, UV_{254} removal reached 86%. Afterward, UV_{254}

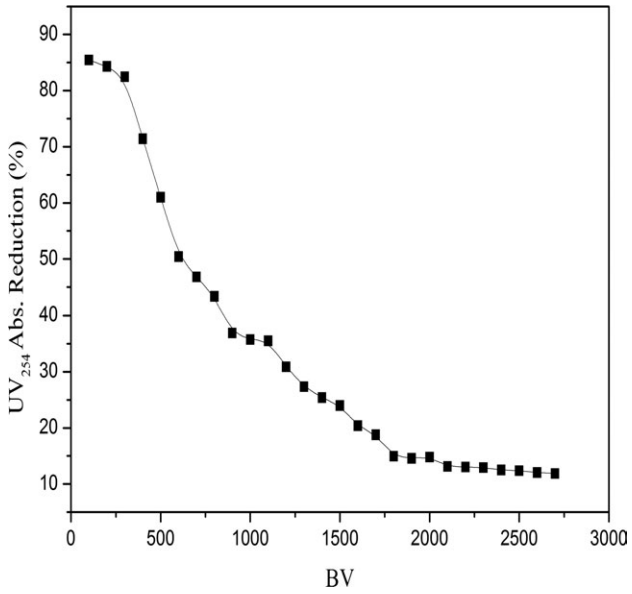

Figure 7. UV_{254} absorbance reduction of m-PGMA multiple-loading tests.

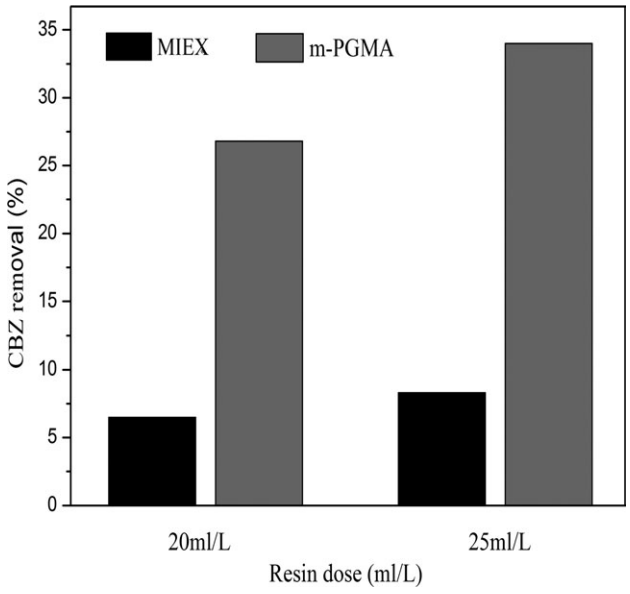

Figure 8. CBZ removal by MIEX® and m-PGMA (resin dose: 20 mL L^{-1} and 25 mL L^{-1}, contact time: 30 min, initial concentration C_0: 200 μg L^{-1}).

removal gradually decreased and reached 18.39% at 1600 BV, after which UV_{254} removal was constant. The strong base anion exchange capacity of m-PGMA is 2.36 mmol g^{-1}, which is similar to the value of MIEX® (2.23 mmol g^{-1}).[33] Moreover, the total PV and the specific SA of m-PGMA were determined to be 0.1852 cm^3 g^{-1} and 40.026 m^2 g^{-1}, respectively. Therefore, multiple-loading tests allow sufficient space, exchange sites, and time for exchanged NOM transport into the interior of m-PGMA. The APD of m-PGMA is approximately 18.5 nm; moreover, m-PGMA is mesoporous and plays a role in transport.

Removal Rate of m-PGMA to CBZ. The objective of the above tests was to compare the CBZ removal efficacy of m-PGMA and MIEX®. The percent removal rates of CBZ that were determined for the two resins are shown in Figure 8. As expected, CBZ, as a nonionic trace organic matter, was found to be poorly removed by MIEX®. Only 6.49% and 8.3% CBZ were removed by MIEX® for 20 mL L^{-1} and 25 mL L^{-1}, respectively, whereas m-PGMA exhibited a higher removal rate of CBZ: approximately 27.8% and 34.7% for 20 mL L^{-1} and 25 mL L^{-1}, respectively. It should be noted that CBZ, as a neutral substance, cannot undergo ion exchange by m-PGMA. Therefore, we attribute the higher removal rate of CBZ to the higher specific SA and PV of m-PGMA compared to MIEX®. Similarly, Suriyanon[33] et al. also determined that those adsorbents with the highest specific SA and PV and the narrowest pore size had the highest adsorption capacity. Both m-PGMA and MIEX® possess these characteristics. It was also reported that hydrogen bonding and hydrophobic interactions are adsorption mechanisms of CBZ onto adsorbents.[33,34] Whether hydrogen bonding and hydrophobic interactions contribute to the adsorption mechanisms of CBZ onto m-PGMA will be discussed in our future work.

CONCLUSIONS

m-PGMA was prepared from magnetic polymer microspheres obtained by the incorporation of oleic-acid-modified and PEG-dispersed magnetite. Mixed porogens were added to increase the specific SA and total PV. The magnetic polymer microspheres reacted with trimethylammonium chloride to obtain quaternary ammonium moieties.

The amount of magnetite in m-PGMA was approximately 6.168 wt %. The specific saturation magnetization of m-PGMA was approximately 10.79 emu g^{-1}, and the coercivity and remanence of m-PGMA were negligible. The specific SA and the total PV of m-PGMA were 40.026 m^2 g^{-1} and 0.1852 cm^3 g^{-1}, respectively. The APD was approximately 18.509 nm, with a narrow pore size distribution.

m-PGMA exhibited fast, efficient removal of NOM due to the well-mixed suspension and small bead size of m-PGMA. After 30 min of contact time, the UV_{254} absorbance reduction increased to 56%, 67%, and 79% for 5, 10, and 15 mL of settled resin L^{-1}, respectively; DOC reduction increased to 53%, 60%, and 72% for 5, 10, and 15 mL settled resin L^{-1}, respectively. In multiple-loading tests, the removal monitored at UV_{254} gradually decreased and reached 18.39% at 1600 BV, after which the removal rate at UV_{254} was constant. After 30 min of contact time, the removal rate of CBZ (200 μg L^{-1}) was 27.8% and 34.7% for 20 mL L^{-1} and 25 mL L^{-1} of m-PGMA, respectively. Compared to MIEX®, m-PGMA has a larger specific SA and PV, which explains why m-PGMA had a better CBZ removal rate compared with MIEX®.

A limitation of this study is that the mechanism for CBZ removal by m-PGMA was not identified. In our future work, we will investigate the mechanisms that determine the removal of CBZ by m-PGMA.

ACKNOWLEDGMENTS

The authors would like to thank Qian Zhang, Wen Chen, and Changlong Dong for their assistance with preparing samples and

performing experiments. The authors also appreciate the support of the Key Laboratory of Integrated Regulation and Resource Development on Shallow Lakes. This research was supported by the National Major Project of Science & Technology Ministry of China (Grant No. 2012ZX07403-001) and by the National Natural Science Foundation of China (No. 51178159).

REFERENCES

1. Matilainen, A.; Vepsäläinen, M.; Sillanpää, M. *Adv. Colloid Interface* **2010**, *159*, 189.
2. David, A. F.; Jenny, B.; Soizic, G.; Carmen, M. E.; Bruce, J.; Derek, W.; Peter, H.; Andrew, T. C.; Simon, A. P. *Water Res.* **2004**, *38*, 2551.
3. Liu, T.; Rao, P.; Lo, I. M. C. *Sci. Total Environ.* **2009**, *407*, 3407.
4. Sharp, E. L.; Jarvis, P.; Parsons, S. A.; Jefferson, B. *Colloids Surf. A: Physicochem. Eng. Aspects* **2006**, *286*, 104.
5. Siva, S.; Madjid, M. *Water Res.* **2010**, *44*, 4087.
6. Humbert, H.; Gallard, H.; Jacquemet, V.; Croué, J. *Water Res.* **2007**, *41*, 3803.
7. Humbert, H.; Gallard, H.; Suty, H.; Croué, J. *Water Res.* **2008**, *42*, 1635.
8. Liu, H.; Liu, R.; Tian, C.; Jiang, H.; Liu, X.; Zhang, R.; Qu, J. *Sep. Purif. Technol.* **2012**, *84*, 41.
9. Ates, N.; Yilmaz, L.; Kitis, M.; Yetis, U. *J. Membr. Sci.* **2009**, *328*, 104.
10. Ambashta, R. D.; Sillanpää, M. J. *Hazard Mater.* **2010**, *180*, 38.
11. Cho, J.; Amy, G.; Pellegrino, J. *Desalination* **2000**, *127*, 283.
12. Ribau, T. M.; Rosa, M. J. *Desalination* **2003**, *151*, 165.
13. Oller, I.; Malato, S.; Sánchez-Pérez, J. A. *Sci. Total Environ.* **2011**, *409*, 4141.
14. Boyer, T. H.; Singer, P. C. *Water Res.* **2005**, *39*, 1265.
15. Boyer, T. H.; Singer, P. C. *Water Res.* **2006**, *40*, 2865.
16. Bolto, B.; Dixon, D.; Eldridge, R.; King, S. *Water Res.* **2002**, *36*, 5066.
17. Drikas, M.; Dixon, M.; Morran, J. *Water Res.* **2011**, *45*, 1539.
18. Pelekani, C.; Snoeyink, V. L. *Water Res.* **1999**, *33*, 1209.
19. Clara, M.; Strenn, B.; Kreuzinger, N. *Water Res.* **2004**, *38*, 947.
20. Im, J.; Cho, I.; Kim, S.; Zoh, K. *Desalination* **2012**, *285*, 306.
21. Xu, W.; Zhang, G.; Zou, S. *Environ. Sci.* **2006**, *27*, 2458 (in Chinese).
22. Humbert, H.; Gallard, H.; Suty, H.; Croué, J. *Water Res.* **2005**, *39*, 1699.
23. Bui, T. X.; Choi, H. J. *Hazard Mater.* **2009**, *168*, 602.
24. Zhang, Y.; Geißen, S.; Gal, C. *Chemosphere* **2008**, *73*, 1151.
25. Bui, T. X.; Choi, H. *Chemosphere* **2010**, *80*, 681.
26. Kitis, M.; Harman, B. I.; Yigit, N. O.; Beyhan, M.; Nguyen, H.; Adams, B. *React. Funct. Polym.* **2007**, *67*, 1495.
27. Lin, C.; Lee, C.; Chiu, W. J. *Colloid Interface. Sci.* **2005**, *291*, 411.
28. Ming, M.; Yu, Z.; Xiaobo, L.; Degang, D.; Huiqian, Z.; Ning, G. *Colloids Surf. A: Physicochem. Eng. Aspects* **2003**, *224*, 207.
29. Ling, Z.; Rong, H.; Hong-chen, G. *Appl. Surf. Sci.* **2006**, *253*, 2611.
30. Yonghoon, L.; Joonho, R.; Bumsuk, J. *J. Appl. Polym. Sci.* **2003**, *89*, 2058.
31. Malgorzata, K.; Katarzyna, M.; Tomasz, W.; Andrew, T. C. *Desalination* **2008**, *221*, 338.
32. Ritchie, J. D.; Perdue, E. M. *Geochim. Cosmochim. Acta.* **2003**, *67*, 85.
33. Suriyanon, N.; Punyapalakul, P.; Ngamcharussrivichai, C. *Chem. Eng. J.* **2013**, *214*, 208.
34. Turku, I.; Sainio, T.; Paatero, E. *Environ. Chem. Lett.* **2007**, *5*, 225.